1772–1784 *Nucleic Acids Research, 2006, Vol. 34, No. 6*
doi:10.1093/nar/gkl106

The DNA–protein interaction modes of FEN-1 with gap substrates and their implication in preventing duplication mutations

Ren Liu[1,2], Junzhuan Qiu[1], L. David Finger[1], Li Zheng[1] and Binghui Shen[1,2,*]

[1]Department of Radiation Biology and [2]Graduate Program in Biological Sciences, City of Hope National Medical Center and Beckman Research Institute, Duarte, CA 91010, USA

Received January 23, 2006; Revised February 14, 2006; Accepted March 8, 2006

ABSTRACT

Flap endonuclease-1 (FEN-1) is a structure-specific nuclease best known for its involvement in RNA primer removal and long-patch base excision repair. This enzyme is known to possess 5′-flap endo- (FEN) and 5′–3′ exo- (EXO) nuclease activities. Recently, FEN-1 has been reported to also possess a gap endonuclease (GEN) activity, which is possibly involved in apoptotic DNA fragmentation and the resolution of stalled DNA replication forks. In the current study, we compare the kinetics of these activities to shed light on the aspects of DNA structure and FEN-1 DNA-binding elements that affect substrate cleavage. By using DNA binding deficient mutants of FEN-1, we determine that the GEN activity is analogous to FEN activity in that the single-stranded DNA region of DNA substrates interacts with the clamp region of FEN-1. In addition, we show that the C-terminal extension of human FEN-1 likely interacts with the downstream duplex portion of all substrates. Taken together, a substrate-binding model that explains how FEN-1, which has a single active center, can have seemingly different activities is proposed. Furthermore, based on the evidence that GEN activity in complex with WRN protein cleaves hairpin and internal loop substrates, we suggest that the GEN activity may prevent repeat expansions and duplication mutations.

INTRODUCTION

Flap endonuclease 1 (FEN-1) is a multifunctional structure-specific nuclease involved in various nucleic acid metabolic pathways (1–3). The enzyme possesses 5′-flap endo- (FEN) and 5′–3′ exonuclease (EXO) activities that are critical for RNA primer removal during lagging strand DNA synthesis and long-patch base excision repair (lpBER) (4–6). In addition, some evidence suggests that FEN-1 is involved in HIV replication (7), non-homologous end joining repair (8), suppression of short sequence recombination (9) and homologous recombination (10). A *RAD27* (FEN-1 homolog) null mutation in *Saccharomyces cerevisiae* results in retarded growth and increased sensitivity to methyl methanesulfonate, which are consistent with the role of FEN-1 in DNA replication and repair (11,12). In addition, the *RAD27* null mutants display a strong mutator phenotype in that the duplication mutations are significantly increased and tracts of repetitive sequences become highly unstable (13–17).

Studies in *Caenorhabditis elegans* surprisingly revealed that the FEN-1 homolog (CRN-1) promotes apoptotic DNA degradation in collaboration with the EndoG homolog CPS-6, which is a mitochondrial endonuclease known to be involved in apoptotic DNA fragmentation (18). Besides the previously described FEN and EXO nuclease activities, CeFEN-1 was shown to possess a gap endonuclease activity, which could be stimulated by CeEndoG (CPS-6). Based on these data, CeFEN-1 and CeEndoG were proposed to function cooperatively in apoptotic DNA degradation (18). Recently, human FEN-1 (hFEN-1) was also shown to possess a GEN activity similar to its *C.elegans* counterpart (19). It was shown that hFEN-1 cleaves DNA structures resembling stalled replication forks using its GEN activity. In addition, the Werner syndrome protein (WRN), which is a RecQ helicase family protein known to stimulate the FEN and EXO activities of hFEN-1, was shown to stimulate the GEN activity of hFEN-1 to cleave stalled replication fork substrates. Further studies in yeast demonstrated that the UV irradiation sensitivity of *rad27* null mutant was alleviated by expression of wild-type hFEN-1, but could not be complemented by the hFEN-1

*To whom correspondence should be addressed. Tel: +1 626 301 8879; Fax: +1 626 301 8280; Email: bshen@coh.org

The authors wish it to be known that, in their opinion, the first two authors should be regarded as joint First Authors

mutants E160D or E178A, which show a deficiency in GEN activity with little effect on the FEN activity (19). Taken together, these results suggested that FEN1 might be involved in break-induced repair of stalled replication forks. Interestingly, FEN-1 expression was shown to be up-regulated in mouse fibroblast cells upon UV exposure in a p53 dependent manner, presumably to assist in stalled replication fork rescue. Furthermore, over-expression of FEN-1 can rescue p53-deficient cells from UV exposure (20).

The X-ray structure analysis and biochemical studies of FEN-1 have provided some insights into how FEN-1 selects and cleaves its DNA substrates (21–24). The global structure of archaeal and human FEN-1 consists of the nuclease core domain and C-terminal extension (Figure 1). Within the nuclease core domain, three major FEN-1 motifs that mediate interaction with DNA substrates have been identified via site-directed mutagenesis and biochemical analyses (21,25) (Figure 1). The positively charged groove formed by Helix–3Turn–Helix motif (H3TH, containing residues Lys^{244}, Arg^{245}, Lys^{252} and Lys^{254} in hFEN-1) has been identified as the site that binds the duplex DNA downstream from the FEN or EXO cleavage site. The helices and loops on the other side of the active center groove (containing residues Arg^{70}, Lys^{326} and Arg^{327} in hFEN-1) form another positively charged groove that binds to the upstream duplex DNA, which is defined as the duplex portion upstream of the DNA cleavage site. The 3D structure of FEN-1 and FRET analysis suggest that the two duplex DNA arms must kink or bend to bind simultaneously (21). A small hydrophobic pocket near the hydrophobic wedge that stacks with the 3′-face of the upstream duplex DNA interacts with a single nucleotide 3′ flap that can further position the flap substrate, thereby ensuring that FEN-1 cleaves exactly 1 nucleotide (nt) into the downstream duplex (21,26). The final DNA-binding motif within FEN-1 is the 'helical clamp' region (also called 'arch'), which consists mainly of charged and hydrophobic amino acid residues that are thought to mediate the interaction with the single-stranded DNA (ssDNA) flap of 5′-flap DNA substrates (21,22). In the absence of DNA binding, the clamp region is relatively far from the active center and is partly disordered (24). However, the binding of the upstream duplex DNA along with a single-nucleotide 3′ flap to FEN-1 is thought to trigger a conformational change in FEN-1 that results in the disordered loops to form α-helices (21). This is consistent with previous report of increased helical content in FEN-1 upon DNA binding (27). In addition, such a conformational rearrangement is suspected to bring some residues such as Arg^{100} in the clamp region closer to the active center and to allow them to participate in catalysis (25,28). The C-terminal extensions of FEN-1s from archaea to humans contain a conserved short sequence motif (Q-x-x-L-D-x-F-F) that is required for high affinity interaction with proliferating cell nuclear antigen (PCNA) *in vitro*. The C-terminal extension in human FEN-1 was revealed to be also involved in DNA substrate binding (29). However, it is still unclear which part of the DNA substrate the C-terminus interacts.

Although FEN-1 possesses three activities that vary in efficacy, the crystal structures of archaebacterial and human

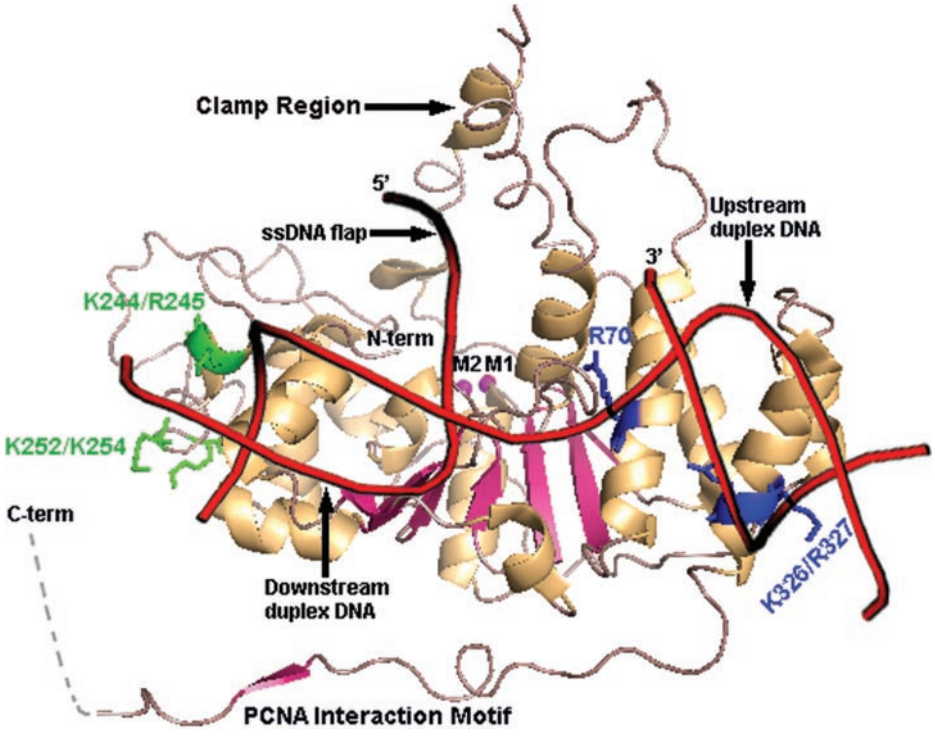

Figure 1. Model of the human FEN-1/double-flap DNA substrate interaction. The structure of human FEN-1 is PDB No. 1UL1 (molecule z) and is shown in a ribbon diagram (24). The β-sheet elements are shown in pink, while α-helices are shown in gold. The two active site metal ions M1 and M2 are shown in magenta. The extreme C-terminus of hFEN-1 is disordered in the crystal structure and represented as a dashed line. DNA is superimposed onto the FEN-1 structure based on previous FEN-1–DNA interaction models (21,25). The region of FEN-1 containing R70 and K326/R327 (shown in blue) interacts with the upstream duplex DNA arm of the substrate. The H3TH motif containing K244/R245 and K252/K254 (shown in green) interacts with the downstream duplex DNA arm of the substrate.

FEN-1 show that FEN-1s have only one active center to perform these various cleavages. How FEN-1 can cleave various substrates and why the three activities vary so widely in efficacy are unknown. In this study, we have sought to determine the reasons for the above questions using extensive kinetic and mutational analysis with various DNA substrates. We have devised a general DNA substrate-binding model that explains how the single active center of FEN-1 can perform cleavage on various substrates. Furthermore, we discuss the effects of the WRN protein on the GEN activity of FEN-1 as an example as to how other proteins can stimulate the relatively weak in vitro activities of FEN-1 to physiologically relevant levels.

MATERIALS AND METHODS

Materials

Human FEN-1 protein and WRN protein expression and purification were performed as described previously (25,30). Protein concentrations were determined by Bradford assay using BSA to generate a standard curve. DNA oligos were synthesized at the City of Hope DNA/RNA/peptide synthesis core facility and purified by denaturing PAGE. The oligo concentrations were determined using A_{260} and calculated extinction coefficients. Oligos used to build various DNA substrates are shown in Table 1.

Three-dimensional structure modeling of hFEN-1/DNA complexes

The hFEN-1 model (Figure 1) was constructed using initial coordinates from the crystal structure of hFEN-1 (Molecule Z) bound to PCNA (PDB code 1UL1) (24). The DNA substrate backbone was then positioned onto the FEN-1 model based on previous DNA–FEN-1 interaction models (21,25). Because the hFEN-1 structure is based on a DNA-free and PCNA-tethered FEN-1 state, this figure is not a precise interaction model.

DNA substrate preparation

DNA substrate preparation was performed as described previously (25). Briefly, oligos were labeled with ddATP at the 3′ end by incubating 40 pmol of the oligo with 15 μCi of [α-^{32}P]ddATP and 1 μl (400 U/μl) of terminal transferase (Roche, Indianapolis, IN) at 37°C for 60 min. The enzyme was then inactivated by heating at 72°C for 10 min. To make substrates, 80 pmol of cold oligos were added to 40 pmol of radiolabled oligo (Table 1 and Figure 2) and heated for 7 min followed by slow cooling to room temperature. Substrates were precipitated by ethanol, washed with 70% ethanol and resuspended in water. The schematic configurations for all the substrates used in this study are shown in Figure 2.

FEN-1 nuclease activity assays

Reactions were carried out with the indicated amount of hFEN-1 and 40 nM DNA substrates in reaction buffer containing 50 mM Tris (pH 8.0) and 10 mM $MgCl_2$, 100 μg/ml BSA and 1 mM DTT in a final volume of 10 μl. Reactions were incubated at 37°C for 15 min and terminated by adding 2 vol of stop-solution (95% formamide, 20 mM EDTA, 0.05% bromophenol blue and 0.05% xylene cyanol). Reactions were analyzed on a 7 M urea, 15% denaturing PAGE in 1× TBE. Gels were dried, and bands were visualized by phosphorimager analysis (Amersham Biosciences, Piscataway, NJ).

Kinetic analyses

Steady-state kinetic studies of human FEN-1 were performed at 37°C under the standard conditions described in the enzyme assay. Varying concentrations of DNA substrates (5, 10, 20, 40 and 80 nM) (final) and a constant amount of FEN1 for each reaction were utilized. Assays were performed at least in triplicate. Reactions were initiated by adding FEN-1 to the reaction mixture, and 10 μl aliquots were removed at 0, 0.5, 1, 1.5, 2 and 2.5 min and immediately mixed with 20 μl of 4°C stop-solution. Under our experimental conditions, the cleavage percentage in each reaction was <10%. The initial velocity was calculated according the equation $v = \mathrm{d}[P]/\mathrm{d}t$, where $[P]$ is the product concentration in nM and t is the reaction time in seconds. The product concentration was calculated by the equation $[P] = \{I_P/(I_S+I_P)\} \times$ [initial substrate], where I_P = product intensity and I_S = remaining substrate intensity. The K_m and V_{max} values were derived from Lineweaver–Burk plot ($1/v \sim 1/s$). k_{cat} was calculated using the equation $k_{cat} = V_{max}/[E]$, where $[E]$ is the enzyme concentration in the reaction. The raw data of kinetic analyses are shown in supplementary figures.

RESULTS

Characterization of FEN-1 GEN activity on various gap substrates

FEN-1 was reported previously to possess a GEN activity on duplex gap substrates (18) and fork gap substrates (19). As shown in Figure 3, FEN-1 activities on these substrates were

Table 1. Oligonucleotides used to build various DNA substrates

Oligo name	Sequences	Used for substrate #
FLAPGT13	5′-GATGTCAAGCAGTCCTAACTTTTTTTTTTTTTTTTGAGGCAGAGTCC-3′	1, 2, 3, 5, 6, 7
FLAPG	5′-GATGTCAAGCAGTCCTAACTTTGAGGCAGAGTCC-3′	4
FBR1G	5′-GGACTCTGCCTCAAGACGGTAGTCAACGTG-3′	1, 2, 6, 7, 8
SHEN14	5′-GGACTCTGCCTCAA-3′	3, 4, 5, 7
FLAP3B	5′-CACGTTGACTACCGTC-3′	2
FLAP3B1	5′-CACGTTGACTACCGTCG-3′	1, 6, 8
FLAPG1CS	5′-AGTTAGGACTGCTTGACATC-3′	4, 5, 6, 7
FPG10	5′-CTTGACATCATACAGTATGATGTCAAGCAGTCCTACTTTGAGGCAGAGTCC-3′	8
LT24	5′-ACCAGCACTGACCCATTAGGGTTTTTTTTTTTTTTTTTTTTTTTTTTTTCCGTCCACCCGACGCCTCCTG-3′	9
ILT1	5′-CAGGAGGCGTCGGGTGGACGGTCCCTAATGGGTCAGTGCTGGT-3′	9

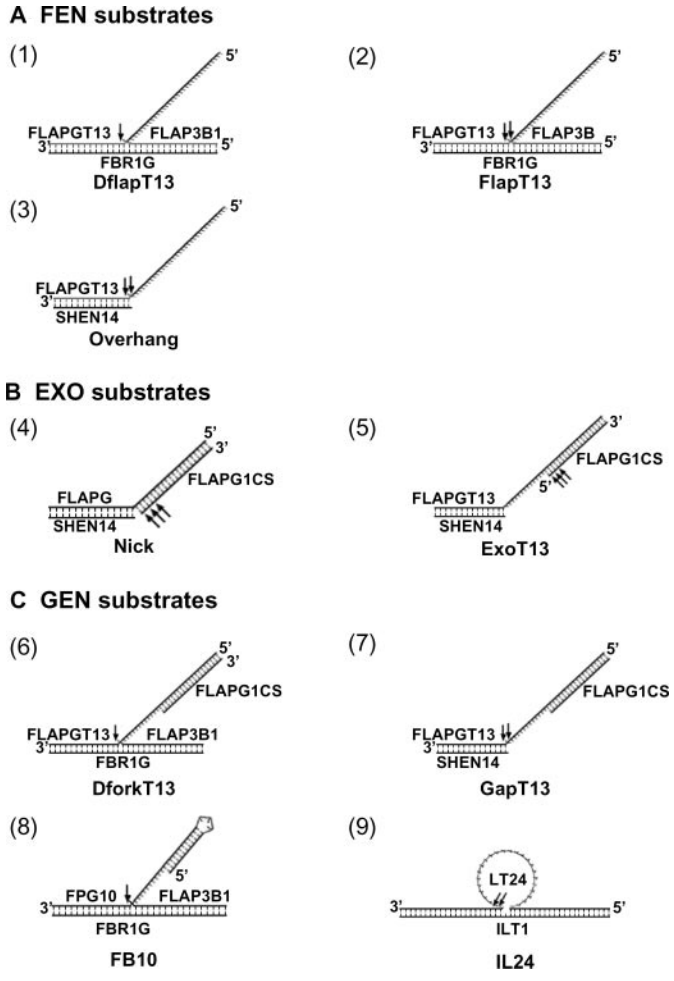

Figure 2. Schematics of three categories of DNA substrates used in this study. The DNA substrates (1–9) for FEN, EXO and GEN activities are shown in (**A**), (**B**) and (**C**), respectively. The arrows indicate the cleavage sites on the DNA substrates. The names of the oligos that correspond to Table 1 are also shown.

compared with the well-characterized FEN and EXO activities. FEN-1 cleavage efficiency is DflapT13 > DforkT13 > ExoT13 > GapT13. As can be seen using the ExoT13 substrate, the 5′–3′ EXO activity of FEN-1 processively digests the downstream primer (downstream and upstream are defined based on the cleavage site, as mentioned previously), but stops when the downstream duplex is 10 bp. This suggests that FEN-1 has a minimum length requirement for the downstream duplex DNA region when performing exonuclease activity (Figure 1). If the ^{32}P-radiolabel on the ExoT13 substrate is changed to the template strand (i.e. GapT13), it is observed that FEN-1 utilizes a GEN activity that is less efficient than EXO activity. Therefore, FEN-1, which has only one active center, has two different activities varying in efficacy on a single DNA substrate (ExoT13 and GapT13; Figure 2B and C).

Parrish *et al*. (18) reported that *C.elegans* FEN-1 displays better GEN activity on gap substrates having a gap size of 4 nt compared with 2 or 1 nt gap substrates. Because only a few gap sizes were assayed, we sought to more comprehensively determine the effect of gap size on the GEN activity of human FEN-1. We designed two series of substrates (duplex gap substrates and fork gap substrates, Figure 4A and B) that have fixed duplex DNA arms and gap lengths that vary with the number of dTs between the duplex arms. Preparing the substrates in this way ensures that the duplex stability is constant with increasing gap size. Using equivalent amounts of FEN-1 in each reaction while varying the gap size of the substrate, the efficiency of GEN activity increases with gap size (Figure 4A and B). These results indicate that FEN-1's GEN activity is more efficient on GEN substrates with larger ssDNA region. Interestingly, the cleavage site is always at the ssDNA/double-stranded DNA (dsDNA) junction for both series of substrates regardless of the length of the gap. In addition, for the duplex gap substrates, the cleavage sites are restricted to one of the two ssDNA/dsDNA junctions, which indicates that FEN-1 still selects the ssDNA region with 5′–3′ polarity similar to that observed with FEN activity. Based on these observations, we conclude that cleavage site selection of fork gap and duplex gap substrate is similar to that of the flap (Figure 3) and 5′-overhang substrates (25), respectively. This further suggests that the ssDNA region of GEN substrates might interact with the clamp region of FEN-1, which is predicted to interact with ssDNA flap of FEN substrates (21).

Comparison of the steady-state kinetic parameters of FEN-1 with various FEN, EXO and GEN substrates

To understand why the cleavage efficiency of FEN-1 activities (FEN, EXO and GEN) varies so much, we performed steady-state kinetic analyses of FEN-1 with DflapT13, FlapT13, Overhang, Nick, ExoT13, DforkT13 and GapT13 substrates (Figure 2, substrates 1–7) by varying substrate concentration (5–80 nM for all substrates) while holding the FEN-1 concentration constant. The k_{cat} value reported here is comparable with other DNA repair nucleases, such as *Sulfolobus solfataricus* Hje endonuclease (31), *Escherichia coli* endonuclease III and formamidopyrimidine glycosylase (32). However, it is faster than the k_{cat} of FEN-1 reported before (25,33,34). This can be explained by the fact that different reaction buffer and temperature are used in these kinetic assays.

As shown in Table 2, the k_{cat} values for DflapT13, FlapT13 and DforkT13 substrates are similar, suggesting that with these substrates, the enzyme can perform cleavage optimally. However, the K_m value of fork gap substrate (DforkT13) is 29 times greater than DflapT13 (Table 2), which likely accounts for the decreased cleavage efficiency (Figure 3). We do note that there is a small change in k_{cat} between DforkT13 and DgapT13 that is outside of the range of error, but it is likely only a minor reason for the difference in cleavage efficiency between the two substrates. The 5′-overhang substrate (Overhang), which is missing the upstream duplex of DflapT13, has a K_m value 32 times greater. This highlights the importance of the interaction of FEN-1 with upstream duplex DNA in substrate binding. As can be seen by comparing the K_m for Nick and FlapT13 substrates, the loss of the 5′-ssDNA flap increases the K_m, which indicates that contacts between FEN-1 and the 5′-ssDNA flap stabilize the FEN-1/flap-DNA complex. In addition, the k_{cat} value for overhang and EXO substrates is much smaller than the value for flap substrates. It is worth noting that the downstream duplex portion in FEN-1 substrates, which is defined as downstream

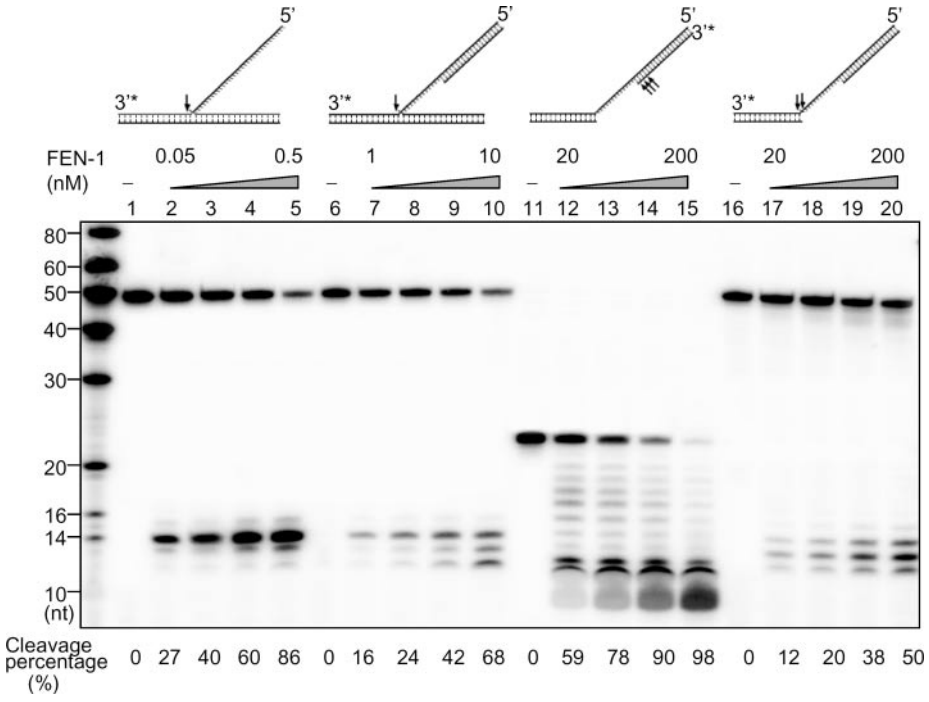

Figure 3. Various biochemical activities of FEN-1. The relative levels of FEN, EXO and GEN activites were tested on four DNA substrates: DflapT13, DforkT13, ExoT13 and GapT13. Enzyme concentrations used are no enzyme for lanes 1, 6, 11 and 16; 0.05, 0.1, 0.2 and 0.5 nM for lanes 2–5; 1, 2, 4 and 10 nM for lanes 7–10; 20, 40, 80 and 200 nM for lanes 12–15; 20, 40, 80 and 200 nM for lanes 17–20. The cleavage percentage $[I_p/(I_p + I_s)]$ for each lane is shown at the bottom.

to the cleavage site, is by definition indispensable. Thus, optimal FEN-1 catalysis and DNA binding requires interaction with three major DNA elements: 5′-ssDNA flap, upstream duplex and downstream duplex.

Interestingly, the ExoT13 and GapT13 substrates are the same structures that only differ in the position of the ^{32}P-radiolabel, but our kinetic analyses show that these two substrates are 15-fold different in K_m value although they are similar in k_{cat}, indicating that the difference in the ability of the protein to bind these substrates accounts for the difference in cleavage efficiency. In fact, there are two different binding modes of FEN-1 with this substrate as will be demonstrated and discussed below.

Site-directed mutagenesis studies of FEN-1 to determine how gap substrates bind

In a previous study, we mutated 28 positively charged amino acids on the surface of human FEN-1 to identify key residues that are involved in the interaction with flap and nick substrates (25). Residues R70 and K326/R327 are in the region of FEN-1 that interact with the upstream duplex DNA of flap and nick substrates. Residues K244/R245 and K252/K254 are part of the H3TH motif, which interacts with downstream duplex DNA of flap and nick substrates (Figure 1) (21). Here, we use the same strategy to determine how FEN-1 binds to GEN substrates. Four DNA-binding-deficient FEN-1 mutants (R70A, K326A/R327A, K244A/R245A and K252A/K254A) were used in cleavage assays with DflapT13, DforkT13, ExoT13 and GapT13 substrates (Figure 5A). As discussed above, the ssDNA region of the gap substrates possibly interacts with the clamp region of FEN-1. If this hypothesis is correct, FEN-1 should bind to the fork gap substrate DforkT13 and double-flap substrate DflapT13 similarly, and mutations that alter DNA binding should affect FEN-1's activity on these two substrates similarly. As shown in Figure 5A, for DflapT13 and DforkT13 substrates, all mutants show deficiency in cleavage, indicating that the upstream and downstream duplex binding regions are important for the interaction with both substrates. This is consistent with our hypothesis that FEN-1 binds DforkT13 and DflapT13 similarly (Figure 5B). In addition, all four mutants show decreased activity with ExoT13 substrate like that seen with the nick substrate (25), suggesting that FEN-1 binds the up- and downstream duplex arms of the ExoT13 like the nick substrate (Figure 5B). For the duplex gap substrate GapT13, we hypothesized that in addition to binding like an EXO substrate (ExoT13), the GapT13 substrate can bind FEN-1 in a manner similar to DforkT13. This alternative mode of binding places the ssDNA region of GapT13 in the helical clamp region and the downstream duplex arm on the H3TH motif of FEN-1. As can be seen in the model (Figure 5B), this orientation retains the 5′–3′ polarity of the ssDNA region in the helical clamp and explains ssDNA/dsDNA cleavage site selection. In addition, when GapT13 is bound in this orientation, the substrate is analogous to the 5′-overhang substrate (Figure 2A), for which cleavage is not affected by FEN-1 mutations in the upstream duplex DNA binding region (25). Mutation of R70 and K326/R327, but not K252/K254 and K244/R245, did not impair the cleavage on GapT13 substrate (Figure 5A), thereby supporting our binding model for the GapT13 substrate with FEN-1. Thus, the duplex gap substrate, which can be cleaved as GEN or EXO substrate by FEN-1, has two modes to bind to FEN-1 (Figure 5B). In one mode (EXO mode), the duplex DNA arms bind the dsDNA-binding

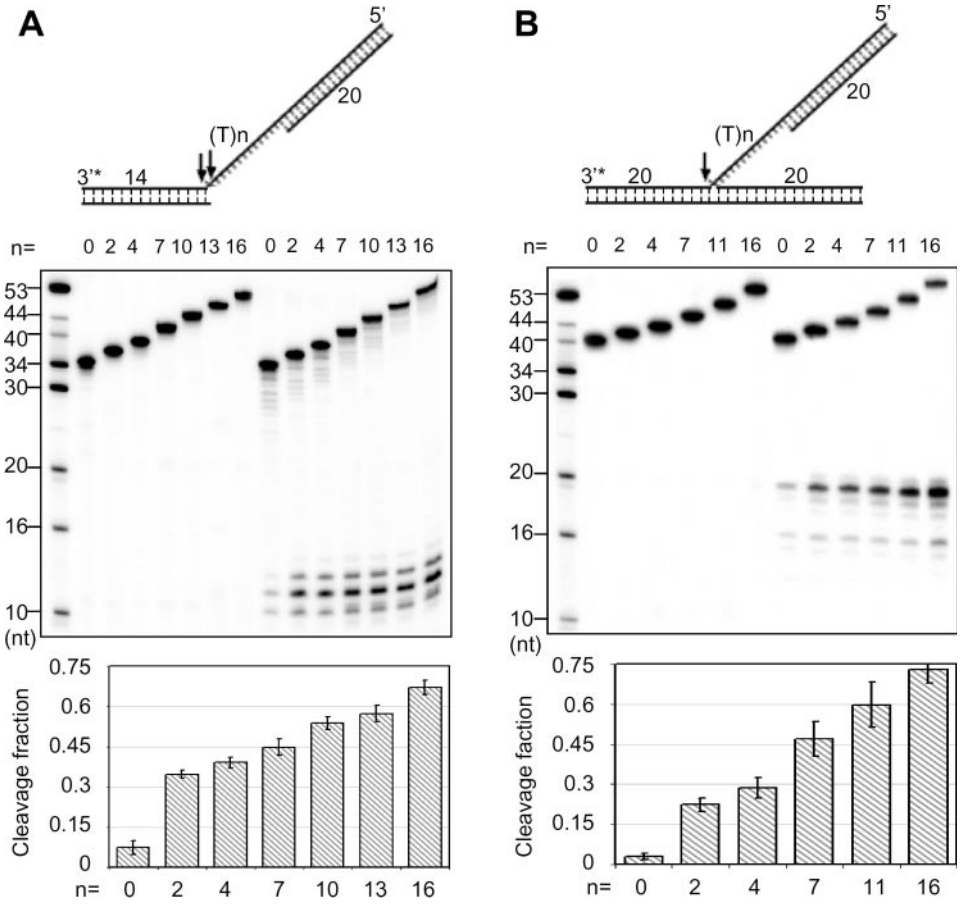

Figure 4. The GEN activity of hFEN-1 increases with increasing gap size. The duplex gap substrates (**A**) and the fork gap substrates (**B**) of various gap sizes were used to determine the optimal gap length for GEN activity. Gap size increases were accomplished by adding the specified number of dTs where indicated. The gap sizes for duplex gap substrates are 0, 2, 4, 7, 10, 13 and 16. The gap sizes for fork gap substrates are 0, 2, 4, 7 11 and 16. The final FEN-1 concentrations in the reactions in (A and B) were 100 and 8 nM, respectively. The bar graph below represents the relative cleavage fraction for each substrate and is an average of three independent experiments.

elements of FEN-1 (R70/K326/R327 element and H3TH motif), thereby placing the 5′ recessed end adjacent to the active center. In another mode (GEN mode), one duplex DNA arm interacts with the H3TH motif, and the ssDNA gap interacts with the helical clamp region, thereby positioning the ssDNA/dsDNA junction adjacent to the active center.

The C-terminus stabilizes the interaction of FEN-1 with the downstream duplex of DNA substrates

The C-terminus of FEN-1 is rich in positively charged residues and has been shown to participate in DNA binding (29). We hypothesized previously that C-terminal tail interacts with the upstream duplex DNA arm of substrates (25). We rationalized that if the C-terminus interacts with the upstream duplex of DNA substrates, then removal of the C-terminal tail should affect cleavage on all substrates except GapT13. Here, we constructed several FEN-1 C-terminal deletion mutants (Figure 6A), and assayed for the ability to cleave all four substrates as above. As shown in Figure 6B, progressive deletion of the C-terminus of FEN-1 adversely affects cleavage of all FEN, EXO and GEN substrates. This characteristic is similar to mutations in the H3TH motif; therefore, the FEN-1 C-terminus likely interacts with the downstream duplex portion of substrates *in vitro*.

FEN-1 cleaves hairpin-flap and internal loop DNA substrates

During lagging strand DNA replication, polymerase δ displaces the RNA primer and adjuvant DNA of an Okazaki fragment to create a flap structure. The displaced flap is usually removed very rapidly by FEN-1. However, if the flap contains direct repeat sequences or di-/tri-nucleotide repeats, flaps can sometimes form hairpins and/or internal loop structures (also called bubble structures) by slip-pairing before they are removed (35). If not resolved, these structures can be ligated into the genome leading to duplication mutations. Evidence indicating a critical role for FEN-1 in avoiding duplication mutation came from studies in yeast *RAD27*/*FEN-1* knock-out mutants, which displayed an increase in the number of duplication mutations and tri-nucleotide repeat expansions (13,17). Based on the track-down model, which explains how FEN-1 recognizes flap DNA substrates, it was thought that FEN-1 is unable to cleave hairpin-flaps and internal loop structures due to the lack of a free 5′ end in these structures (36). However, the presence or absence of FEN-1 in yeast cells made significant difference in the stability of triple repeat

Table 2. The kinetic analyses of wide type FEN-1 on different DNA substrates

Activity	DNA substrate	K_m (nM) (fold)	k_{cat}[a] ($\times 10^{-3}$ s^{-1}) (fold)	k_{cat}/K_m ($\times 10^{-3}$ nM^{-1} s^{-1}) (fold)
FEN	(1) DflapT13	3.0 ± 0.3 (1)	181 ± 35 (1)	62 ± 17 (1000)
	(2) FlapT13	15.9 ± 1.8 (5)	137 ± 26 (0.8)	8.6 ± 1.4 (138)
	(3) Overhang	97 ± 14 (32)	11.9 ± 1.5 (0.07)	0.12 ± 0.01 (1.9)
EXO	(4) Nick	93 ± 18 (31)	10.1 ± 2.5 (0.05)	0.11 ± 0.04 (1.8)
	(5) ExoT13	13.7 ± 3.4 (5)	6.9 ± 1.3 (0.04)	0.52 ± 0.08 (8.4)
GEN	(6) DforkT13	86 ± 7 (29)	126 ± 12 (0.7)	1.5 ± 0.2 (24)
	(7) GapT13	226 ± 9 (75)	6.6 ± 0.7 (0.04)	0.029 ± 0.004 (0.5)

[a]k_{cat} values are calculated from the equation $k_{cat} = V_{max}/[E]$. The enzyme concentrations ([*E*]) for substrates (1)–(7) are 0.02, 0.1, 10, 4, 4, 0.4 and 20 nM, respectively.

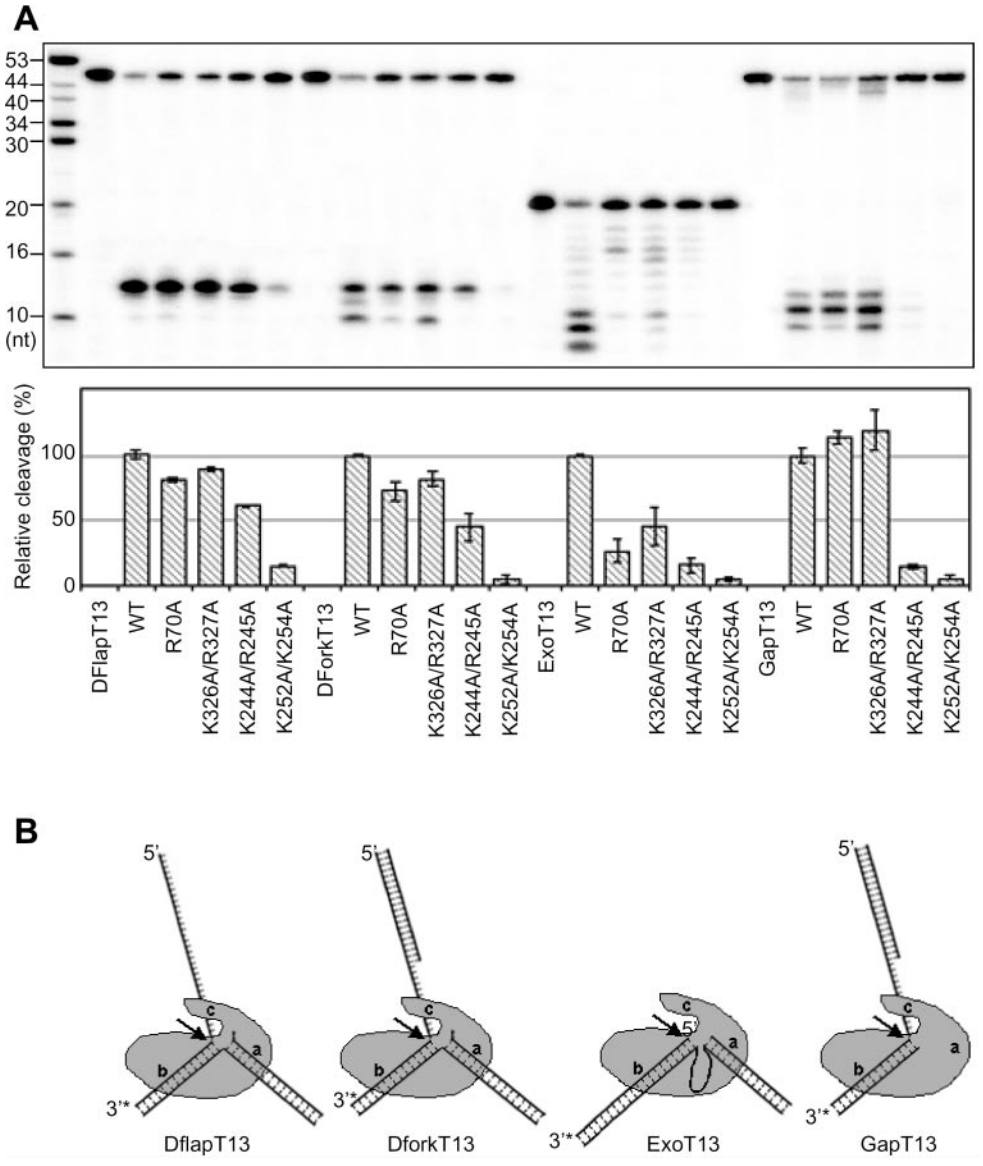

Figure 5. Effects of hFEN-1 DNA-binding deficiency on various substrates. (**A**) Four DNA substrates, DflapT13, DforkT13, ExoT13 and GapT13 were assayed with wild type and mutant hFEN-1 to determine the effects of DNA-binding deficiency on substrate cleavage. The hFEN-1 concentrations used for DflapT13, DforkT13, ExoT13 and GapT13 reactions were 0.5, 15, 100 and 200 nM, respectively. The bar graph below represents the relative cleavage percentage for each substrate (normalized to wild-type enzyme) and is an average of at least three independent experiments. (**B**) Schematic representations of FEN-1 interaction with the four DNA substrates used here. FEN-1 is represented as a gray mitten, and the relative positions of the upstream duplex DNA binding motif, downstream duplex DNA-binding (H3TH) motif and ssDNA-binding motif (helical clamp) are indicated with letters a, b and c, respectively. Arrows indicate where the cleavage of various substrates occurs and are the approximate location of the active center.

sequences (16). This suggests that FEN-1 may have a more active role in the maintenance of triple repeat stability. The GEN activity of FEN-1 is a good candidate mechanism. Therefore, FEN-1 was assayed *in vitro* to determine if it could cleave hairpin-flap and internal loop DNA structures, the intermediate DNA structures in generating duplication mutations. As seen in Figure 7, FEN-1 can cleave, albeit weakly, hairpin-flap and internal loop structures.

The hairpin-flap DNA substrate is similar to the fork gap substrate, except that the end of flap is a hairpin turn instead of a blunt ended duplex. Therefore, it is not surprising that the site and efficiency of FEN-1 cleavage are very similar (Figure 7A). Moreover, as gap size of the hairpin-flap structure increases (i.e. shorten the fold-back length), FEN-1 cleavage efficiency increases as well, similar to that seen with fork gap substrates (Figure 4B). No cleavage on the 5′ end of the hairpin-flap was detected, which rules out the possibility that this cleavage of fork gap substrates resulted from FEN-1 using its 5′–3′ exonuclease activity to processively digest the 5′ end to make an ssDNA flap.

With the internal loop substrate, the site of cleavage is at the ssDNA/dsDNA junction on the 3′ side of the internal loop, which suggests that FEN-1 binds ssDNA loop with 5′–3′ polarity. In addition, owing to the high concentration of FEN-1 necessary to observe cleavage, processive exonucleolytic cleavage occurs post endonucleolytic cleavage (Figure 7B). Previously, FEN-1 was shown to be unable to cleave internal loop structures with <12 nt in the loop. In addition, the ability of FEN-1 to cleave such a substrate increased significantly when the loop size was increased from 12 to 24 nt (37). To further understand how the loop size affects FEN-1 cleavage, we performed FEN-1 assay with substrates of varying loop sizes (24, 36 and 48 nt). The efficiency of FEN-1 cleavage is similar for these three substrates, indicating that FEN-1's activity on internal loop substrates does not increase once the loop size is 24 nt or greater.

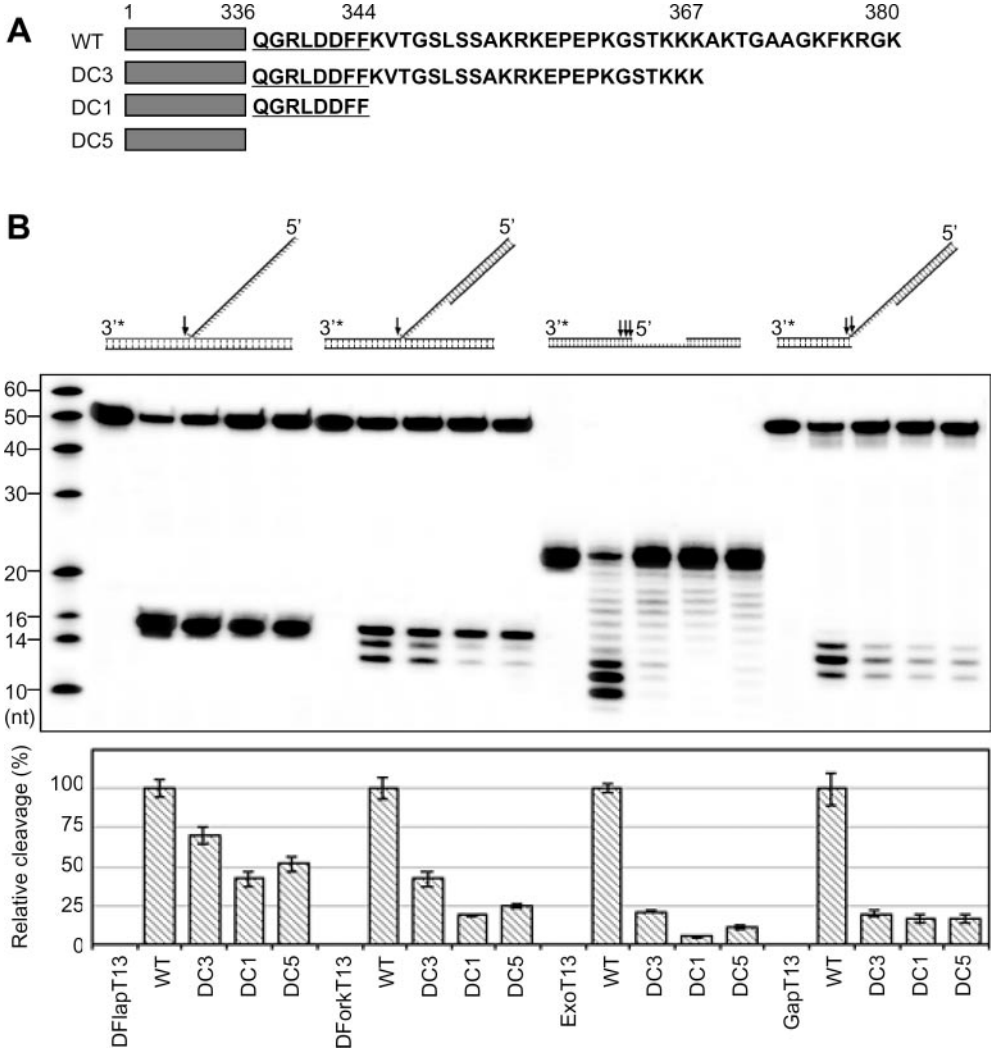

Figure 6. FEN-1 C-terminus interacts with the downstream portion of DNA substrates. (**A**) Sequence of the human FEN-1 C-terminus and deletion mutants thereof. The nuclease core domain is represented as a gray box, and the PCNA interaction motif is underlined. (**B**) The effect of C-terminal deletion mutations on various FEN-1 substrates. The final FEN-1 concentrations for DflapT13, DforkT13, ExoT13 and GapT13 reactions were 0.5, 15, 100 and 200 nM, respectively. The relative cleavage percentage (normalized to wild-type enzyme) is shown in the bar graph below and is an average of at least three independent experiments.

WRN protein significantly stimulated GEN activity on hairpin-flap and internal loop substrates

FEN-1 has been shown to have activities on hairpin-flap and internal loop substrates, although these activities are less efficient compared with FEN activity *in vitro*. FEN-1 is known to interact with 17 different proteins, some of which modulate FEN-1 nuclease activities (3). Therefore, other cellular proteins may facilitate cleavage of substrates *in vivo* that are poor *in vitro* substrates. One such FEN-1 interaction partner is the WRN protein, which has been shown to stimulate FEN-1's activities (FEN, EXO and GEN) *in vitro* (19,30) and to interact with FEN-1 *in vivo* (30). WRN is a RecQ helicase possessing helicase and 3′–5′ exonuclease activities, but its ability to stimulate FEN-1 solely depends on a conserved non-catalytic domain (30). To see if WRN can also stimulate FEN-1's activity on hairpin-flap and internal loop substrates, we performed FEN-1 assays on these DNA substrates with the WRN protein. Because no ATP was included in the reaction and WRN has a very weak exonuclease activity on the DNA with 3′ protruding strand (38), the helicase and exonuclease activity of WRN can be ignored. As shown in Figure 8, WRN significantly stimulates (~10-fold) FEN-1 cleavage on hairpin-flap substrate FB10 to a level similar to the cleavage on double flap substrate DflapT2. FEN-1's activity on internal loop substrate IL36 can also be stimulated by WRN (Figure 8). As a control, BSA did not stimulate cleavage of these substrates (Figure 8). This suggests that the WRN/FEN-1 may be important to resolve aberrant DNA structures that can arise during Okazaki fragment maturation.

DISCUSSION

DNA binding modes and catalytic properties of FEN-1

FEN-1 has long been known as the primary nuclease for RNA-primer/DNA flap removal in Okazaki fragment maturation and lpBER (4–6). Early mechanistic studies suggested that FEN-1 recognizes the free 5′ end of flap substrates and then proceeds to track down the flap to the cleavage site. This track-down model explained how FEN-1 can bypass blocks such as DNA branch and *cis*-diamminedichloroplatinum adducts, but not DNA duplex (39,40). However, recently published work (18,19) and the current study have shown that FEN-1 also possesses a GEN activity. Why GEN activity is weaker than FEN activity on comparable substrates and how EXO and GEN substrates are recognized without a free 5′ end is unknown. Here, we present a model based on kinetic and site-directed mutagenesis data that can explain how flapless structures like EXO and GEN substrates bind FEN-1. In addition, our model explains how an enzyme with a single active center can have seemingly different activities.

Structural studies have revealed that FEN-1 has two dsDNA-binding regions and an ssDNA-binding region (helical clamp). Based on previous work, flap DNA substrates were determined to require all three major DNA binding elements for optimal cleavage (25). Because the EXO substrates (Nick

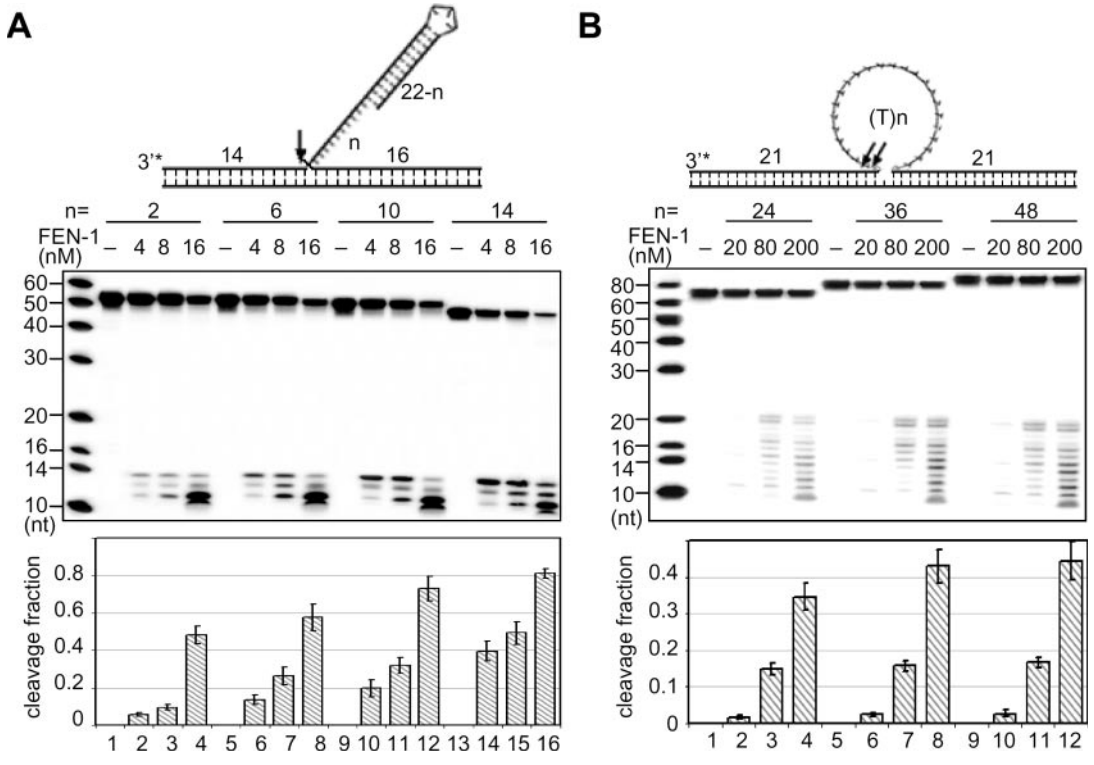

Figure 7. FEN-1 cleaves hairpin-flap and internal loop DNA substrates. (**A**) Substrates with four gap sizes (2,6,10,14) due to flap hairpin formation were assayed with three concentrations (4, 8 and 16 nM) of FEN-1. (**B**) Substrates with three internal loop size (24, 36 and 48 nt) were assayed with three concentrations (20, 80 and 200 nM) of FEN-1. The internal loop size was changed by adding dTs between the two duplex arms. The bar graph below represents the relative cleavage fraction for each substrate and is an average of three independent experiments.

and ExoT13) have no ssDNA 5′-flap, they presumably only need the two duplex DNA-binding regions of FEN-1 for interaction. Owing to the loss of the ssDNA flap interaction, an increased K_m is observed for these substrates compared to the double-flap substrate, suggesting that the ssDNA flap contacts FEN-1 in the helical clamp for optimal affinity. Interestingly, a lower k_{cat} is also observed for EXO substrates when compared with flap or fork substrates (Table 2). As stated before, studies have shown that FEN-1 conformational changes are induced upon DNA binding, especially in the clamp region (21,27). In light of this, the loss of catalytic efficiency suggests that important structural rearrangements occur in the clamp region upon ssDNA binding that are required for optimal catalysis. Interestingly, EXO cleavage is usually one nucleotide into the downstream duplex DNA region, but to a lesser extent di-nucleotide cleavage into the downstream duplex can also be detected, which is similar to that seen for flap substrates lacking the 3′ nt flap (26). In fact, like double flap substrates, addition of a 3′-single nucleotide flap to a nick substrate resulted in complete loss of detectable di-nucleotide cleavage products (26). We suggest that EXO activity may be due to breathing of the terminal base pair such that a single 5′ nt flap enters into the active site for cleavage. Depending on the stability of the duplex, the terminal nucleotide of the downstream duplex may fray and enter the ssDNA binding region resulting in the second nucleotide entering the active site for cleavage. In support of this, the duplex arms are kinked relative to one another (21), and stress due to this conformational change may facilitate formation of a single nucleotide 5′-flap at a nick site similar to that seen with the 3′–5′ exonuclease activity of the Klenow fragment (41). The fact that ExoT13 has smaller K_m value than Nick (Table 2) may also be explained by this mechanism in that ExoT13 has longer flexible ssDNA region and can be more easily kinked.

The GEN activity on the fork DNA substrate used here only differs from the double-flap substrate by the presence of an additional oligo annealed to the flap portion of the DNA. We have proposed that DforkT13 binds FEN-1 in a manner analogous to the flap substrates, and have some evidence to support this from mutational studies (Figure 5B). Unlike EXO and duplex gap substrates, we detected a large difference in the K_m of fork gap substrates in comparison with flap substrates, thereby suggesting that for the most part, the cleavage efficiency of DforkT13 is less due to a decreased binding affinity for this substrate. One reason for this major decrease in binding affinity could be the loss of a free 5′-ssDNA flap. FEN-1 has been proposed to recognize the free 5′ ends of ssDNA on flap structures and track-down to the cleavage site. If FEN-1 is not capable of tracking due to the loss of a ssDNA flap, FEN-1 may utilize a less efficient alternative substrate recognition mode in which dsDNA binding occurs first with the helical arch subsequently clamping onto the ssDNA region of the fork gap substrate. Another possibility to explain the decreased binding affinity is a steric argument in that the dsDNA portion of the flap strand prevents some portion of the ssDNA from binding, thereby causing a loss in affinity. This hypothesis is consistent with our result that GEN activity increases along with the expansion of gap size (Figure 4). In addition, because upon DNA binding, the clamp region undergoes conformational changes, the loss of binding to some portion of the

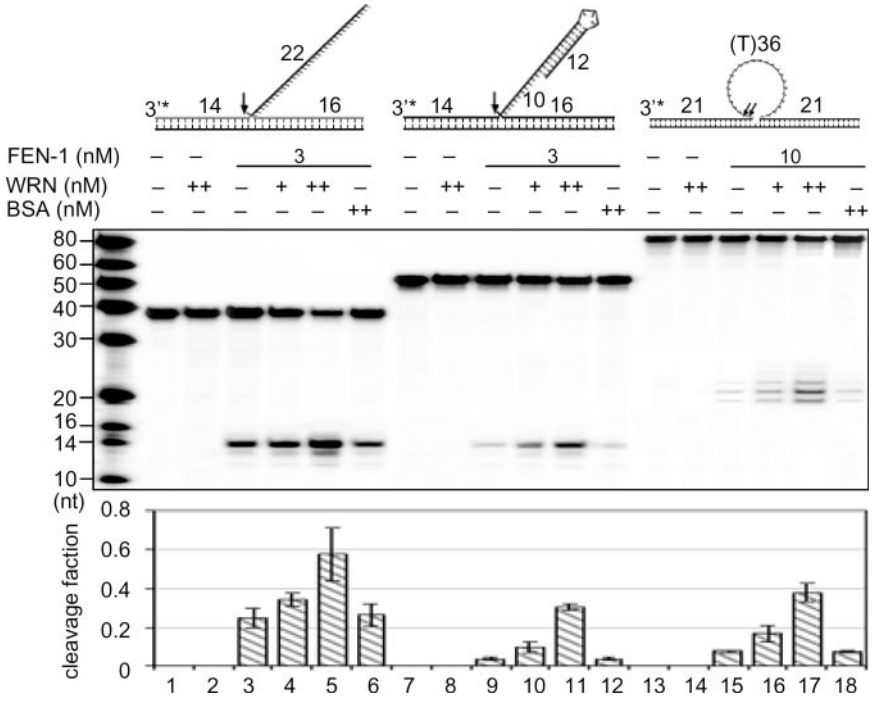

Figure 8. WRN protein stimulates FEN-1 to cleave hairpin-flap and internal loop substrates. The simulation of FEN-1 activity by WRN protein on hairpin-flap DNA FB10 and internal loop DNA IL36 was compared with the stimulation on double flap DNA substrate DflapT2. The FEN-1 concentration was 3, 3 and 10 nM for DflapT2, FB10 and IL36, respectively. Lanes 1, 7 and 13 only has DNA substrates in the reaction. Plus, 100 nM WRN protein. Double plus, 400 nM WRN or BSA. The reaction buffer for stimulation assay contained 50 mM Tris–HCl (pH 8.0), 10 mM $MgCl_2$ and 50 mM NaCl. The bar graph below represents the relative cleavage fraction for each substrate and is an average of three independent experiments.

ssDNA may also prevent all the necessary conformational rearrangements for optimal catalysis or affect substrate positioning, thereby explaining the small change in k_{cat}. Another possibility for the decrease in observed affinity is that instead of two dsDNA duplexes for two dsDNA-binding motifs, fork gap substrates, which have three dsDNA duplexes, may bind in more than one manner and hence decrease the observable cleavage. In support of this, we have seen that depending on the position of the label (i.e. labeling the 5′ end of the oligo annealed to the flap portion), EXO activity can be observed on the same substrate (data not shown).

The GEN activity on duplex gap substrates is the weakest activity of FEN-1. Kinetic characterization of duplex gap cleavage has revealed that the binding affinity of FEN-1 for this type of substrate is the poorest, while the k_{cat} is comparable with the EXO activity and FEN activity on 5′-overhang substrates. Based on our mutational data and by analogy to 5′-overhang and fork gap substrates, we have proposed that duplex gap substrates bind the helical clamp and H3TH motif of FEN-1 (Figure 5B). Thus, loss of binding affinity can be easily explained due to loss of interaction with the upstream duplex DNA-binding region of FEN-1 similar to that seen for 5′-overhang substrates. In addition, the duplex on the flap-like portion of the substrate may prevent optimal binding in a manner similar to that proposed for fork gap substrates. Furthermore, the decrease in the k_{cat} can be rationalized similarly to the 5′-overhang substrate in that conformational rearrangements necessary for optimal catalysis do not occur due to loss of binding to the upstream duplex DNA-binding motif.

By comparing the substrate specificity constant k_{cat}/K_m (Table 2), the best substrate for FEN-1 is the double-flap structure, consistent with the crucial roles of FEN-1 in Okazaki fragment maturation and lpBER. The fork gap substrate used here, which to some degree mimics a stalled replication fork, is not as favored as the flap substrates. The least favored substrate is duplex-gap DNA, which is proposed to be the substrate of FEN-1 in apoptotic DNA fragmentation (18). Considering that high levels of FEN-1 GEN activity would likely create dsDNA breaks *in vivo*, it is probably beneficial that this enzyme is an inefficient gap endonuclease. FEN-1 may require the assistance of other proteins like WRN (19) or EndoG (18) to facilitate GEN activity on stalled replication forks and duplex gap substrates, respectively.

The role of the extreme C-terminus of FEN-1 in substrate binding

We have shown that the C-terminus of FEN-1 likely interacts with the downstream DNA duplex *in vitro*. Because the PCNA interaction site on FEN-1 is a portion of the C-terminus, whether the C-terminus participates in DNA binding when bound to PCNA *in vivo* is questionable. Stucki, *et al*. reported that removal of the last 21 amino acids of human FEN-1 did not affect FEN-1/PCNA binding, but did adversely affect FEN-1 cleavage assays in the presence of PCNA and FEN-1/DNAbinding assays, suggesting that even when PCNA is present, the extreme C-terminus of FEN-1 influences substrate binding (29). Whether the FEN-1/PCNA and FEN-1 C-terminus/DNA interactions can occur simultaneously remains to be shown. Recent data from the Cardoso lab suggest that FEN-1 is only transiently associated with PCNA at replication foci (42). Therefore, FEN-1 is likely loaded onto PCNA for flap removal and then dissociates very rapidly once it has cleaved the flap. The FEN-1/PCNA co-crystal structure contained three conformational states of the FEN-1/PCNA interaction. The conformation displaying the most protein–protein interaction was the inactive state, in which FEN-1 is likely very distant form the DNA substrate. The other two conformations of FEN-1, which result from rotation about a hinge region, showed that FEN-1 was captured in a conformation that may represent an intermediate to DNA binding. These conformations, which are likely more similar to the active form of FEN-1, had less protein–protein contacts with PCNA, suggesting that FEN-1/substrate binding may be coupled to the release of the C-terminus from PCNA. Therefore, the C-terminus may be able to interact with the downstream duplex DNA *in vivo*. It should also be noted that the extreme C-terminus of FEN-1 is acetylated *in vitro* and *in vivo* on lysine residues, and this modification does affect FEN-1 cleavage and substrate binding *in vitro* (43). Furthermore, the extreme C-terminus of FEN-1 has been reported to interact with WRN and BLM (44). Therefore, how these functions of FEN-1 C-terminus coordinate *in vivo* needs further investigation.

The implication of the involvement of FEN-1/WRN in preventing duplication mutations

Certain sequences can form stable secondary structures (hairpins or loops) *in vivo* and inhibit the DNA replication machinery (45). Since FEN-1 was originally thought to only be able to bind substrates having free 5′-ssDNA ends, FEN-1 was thought to be unable to remove these structures. Therefore, the dramatically increased duplication mutation and tri-nucleotide expansion rate observed in *RAD27* null mutant (13,17) were explained by the greatly increased life-time of flaps *in vivo* (35). In this study, we show that FEN-1 alone can weakly cleave hairpin and internal loop substrates. In addition, the cleavage of these substrates can be significantly stimulated by WRN (Figure 8), thereby implicating the FEN-1/WRN complex in the removal of aberrant DNA structures that can form during Okazaki fragment maturation. Ruggiero and Topal (46) reported that FEN-1 cannot cleave the hairpin and bubble structures formed by GAA repeat sequences *in vitro*. However the substrates in their assays were only labeled at the 5′ end, which makes the endonuclease cleavage undetectable because FEN-1's 5′ exonuclease activity removes the radiolabeled base. We must admit that the GEN activity is indeed much weaker than the FEN activity in *in vitro* assays. We suggest that with the stimulation by other protein partners such as WRN (Figure 8), the GEN activity of FEN-1 might be relevant *in vivo*. In support of this, the non-catalytic WRN C-terminus (RQC) domain, which is responsible for FEN-1 activity stimulation, has been shown to rescue a temperature-sensitive *dna2* mutant *in vivo*, presumabaly via stimulation of FEN-1 activity (47). Some evidences also suggest that WRN and FEN-1 are present in replication foci and recruited to stalled replication forks (19,48). How WRN stimulates FEN-1 on substrates is not well understood. However, the RQC domain binds to DNA (49), and its DNA-binding properties are crucial for stimulation of FEN-1 (50). Therefore, RQC domain may facilitate

FEN-1 cleavage by loading the GEN substrates onto FEN-1 and/or stabilizing the enzyme/substrate complex. Pre-steady and steady-state kinetic studies investigating the effect of this domain on FEN-1 activities should shed light on this possibility.

The Bloom Syndrome protein (BLM), a RecQ helicase closely related to WRN, has also been shown to assist FEN-1 in the resolution of hairpin and internal loop structures (37). Although BLM can stimulate FEN-1 cleavage on these substrates in the absence of helicase activity, the helicase activity of BLM can further increase the cleavage efficiency of FEN-1. Therefore, Wang and Bambara (37) proposed a sequential mechanism in which BLM resolves aberrant DNA secondary structures first with subsequent removal of the flap by FEN-1. In light of this, the RQC domain and the helicase domain of WRN may also work together to help FEN-1 remove aberrant DNA structures formed during Okazaki fragment maturation, thereby avoiding duplication mutations and repeat expansions.

SUPPLEMENTARY DATA

Supplementary Data are available at NAR Online.

ACKNOWLEDGEMENTS

We thank the members of the Shen laboratory and Dr Gerald Wuenschell for technical assistance and stimulating discussions. This work was supported by NCI, National Institutes of Health Grant R01CA073764 to B.H.S. Funding to pay the Open Access publication charges for this article was provided by NIH.

Conflict of interest statement. None declared.

REFERENCES

1. Harrington,J.J. and Lieber,M.R. (1994) The characterization of a mammalian DNA structure-specific endonuclease. *EMBO J.*, **13**, 1235–1246.
2. Liu,Y., Kao,H.I. and Bambara,R.A. (2004) Flap endonuclease 1: a central component of DNA metabolism. *Annu. Rev. Biochem.*, **73**, 589–615.
3. Shen,B., Singh,P., Liu,R., Qiu,J., Zheng,L., Finger,L.D. and Alas,S. (2005) Multiple but dissectible functions of FEN-1 nucleases in nucleic acid processing, genome stability and diseases. *Bioessays*, **27**, 717–729.
4. Kim,K., Biade,S. and Matsumoto,Y. (1998) Involvement of flap endonuclease 1 in base excision DNA repair. *J. Biol. Chem.*, **273**, 8842–8848.
5. Turchi,J.J., Huang,L., Murante,R.S., Kim,Y. and Bambara,R.A. (1994) Enzymatic completion of mammalian lagging-strand DNA replication. *Proc. Natl Acad. Sci. USA*, **91**, 9803–9807.
6. Waga,S., Bauer,G. and Stillman,B. (1994) Reconstitution of complete SV40 DNA replication with purified replication factors. *J. Biol. Chem.*, **269**, 10923–10934.
7. Rumbaugh,J.A., Fuentes,G.M. and Bambara,R.A. (1998) Processing of an HIV replication intermediate by the human DNA replication enzyme FEN1. *J. Biol. Chem.*, **273**, 28740–28745.
8. Wu,X., Wilson,T.E. and Lieber,M.R. (1999) A role for FEN-1 in nonhomologous DNA end joining: the order of strand annealing and nucleolytic processing events. *Proc. Natl Acad. Sci. USA*, **96**, 1303–1308.
9. Negritto,M.C., Qiu,J., Ratay,D.O., Shen,B. and Bailis,A.M. (2001) Novel function of Rad27 (FEN-1) in restricting short-sequence recombination. *Mol. Cell. Biol.*, **21**, 2349–2358.
10. Kikuchi,K., Taniguchi,Y., Hatanaka,A., Sonoda,E., Hochegger,H., Adachi,N., Matsuzaki,Y., Koyama,H., van Gent,D.C., Jasin,M. *et al.* (2005) Fen-1 facilitates homologous recombination by removing divergent sequences at DNA break ends. *Mol. Cell. Biol.*, **25**, 6948–6955.
11. Reagan,M.S., Pittenger,C., Siede,W. and Friedberg,E.C. (1995) Characterization of a mutant strain of *Saccharomyces cerevisiae* with a deletion of the RAD27 gene, a structural homolog of the RAD2 nucleotide excision repair gene. *J. Bacteriol.*, **177**, 364–371.
12. Sommers,C.H., Miller,E.J., Dujon,B., Prakash,S. and Prakash,L. (1995) Conditional lethality of null mutations in RTH1 that encodes the yeast counterpart of a mammalian 5′- to 3′-exonuclease required for lagging strand DNA synthesis in reconstituted systems. *J. Biol. Chem.*, **270**, 4193–4196.
13. Callahan,J.L., Andrews,K.J., Zakian,V.A. and Freudenreich,C.H. (2003) Mutations in yeast replication proteins that increase CAG/CTG expansions also increase repeat fragility. *Mol. Cell. Biol.*, **23**, 7849–7860.
14. Freudenreich,C.H., Kantrow,S.M. and Zakian,V.A. (1998) Expansion and length-dependent fragility of CTG repeats in yeast. *Science*, **279**, 853–856.
15. Ireland,M.J., Reinke,S.S. and Livingston,D.M. (2000) The impact of lagging strand replication mutations on the stability of CAG repeat tracts in yeast. *Genetics*, **155**, 1657–1665.
16. Spiro,C., Pelletier,R., Rolfsmeier,M.L., Dixon,M.J., Lahue,R.S., Gupta,G., Park,M.S., Chen,X., Mariappan,S.V. and McMurray,C.T. (1999) Inhibition of FEN-1 processing by DNA secondary structure at trinucleotide repeats. *Mol. Cell*, **4**, 1079–1085.
17. Tishkoff,D.X., Filosi,N., Gaida,G.M. and Kolodner,R.D. (1997) A novel mutation avoidance mechanism dependent on *S.cerevisiae* RAD27 is distinct from DNA mismatch repair. *Cell*, **88**, 253–263.
18. Parrish,J.Z., Yang,C., Shen,B. and Xue,D. (2003) CRN-1, a *Caenorhabditis elegans* FEN-1 homologue, cooperates with CPS-6/EndoG to promote apoptotic DNA degradation. *EMBO J.*, **22**, 3451–3460.
19. Zheng,L., Zhou,M., Chai,Q., Parrish,J., Xue,D., Patrick,S.M., Turchi,J.J., Yannone,S.M., Chen,D. and Shen,B. (2005) Novel function of the flap endonuclease 1 complex in processing stalled DNA replication forks. *EMBO Rep.*, **6**, 83–89.
20. Christmann,M., Tomicic,M.T., Origer,J. and Kaina,B. (2005) Fen1 is induced p53 dependently and involved in the recovery from UV-light-induced replication inhibition. *Oncogene*, **24**, 8304–8313.
21. Chapados,B.R., Hosfield,D.J., Han,S., Qiu,J., Yelent,B., Shen,B. and Tainer,J.A. (2004) Structural basis for FEN-1 substrate specificity and PCNA-mediated activation in DNA replication and repair. *Cell*, **116**, 39–50.
22. Hosfield,D.J., Mol,C.D., Shen,B. and Tainer,J.A. (1998) Structure of the DNA repair and replication endonuclease and exonuclease FEN-1: coupling DNA and PCNA binding to FEN-1 activity. *Cell*, **95**, 135–146.
23. Hwang,K.Y., Baek,K., Kim,H.Y. and Cho,Y. (1998) The crystal structure of flap endonuclease-1 from *Methanococcus jannaschii*. *Nature Struct. Biol.*, **5**, 707–713.
24. Sakurai,S., Kitano,K., Yamaguchi,H., Hamada,K., Okada,K., Fukuda,K., Uchida,M., Ohtsuka,E., Morioka,H. and Hakoshima,T. (2005) Structural basis for recruitment of human flap endonuclease 1 to PCNA. *EMBO J.*, **24**, 683–693.
25. Qiu,J., Liu,R., Chapados,B.R., Sherman,M., Tainer,J.A. and Shen,B. (2004) Interaction interface of human flap endonuclease-1 with its DNA substrates. *J. Biol. Chem.*, **279**, 24394–24402.
26. Friedrich-Heineken,E. and Hubscher,U. (2004) The Fen1 extrahelical 3′-flap pocket is conserved from archaea to human and regulates DNA substrate specificity. *Nucleic Acids Res.*, **32**, 2520–2528.
27. Kim,C.Y., Park,M.S. and Dyer,R.B. (2001) Human flap endonuclease-1: conformational change upon binding to the flap DNA substrate and location of the Mg2+ binding site. *Biochemistry*, **40**, 3208–3214.
28. Allawi,H.T., Kaiser,M.W., Onufriev,A.V., Ma,W.P., Brogaard,A.E., Case,D.A., Neri,B.P. and Lyamichev,V.I. (2003) Modeling of flap endonuclease interactions with DNA substrate. *J. Mol. Biol.*, **328**, 537–554.
29. Stucki,M., Jonsson,Z.O. and Hubscher,U. (2001) In eukaryotic flap endonuclease 1, the C terminus is essential for substrate binding. *J. Biol. Chem.*, **276**, 7843–7849.
30. Brosh,R.M.Jr, von Kobbe,C., Sommers,J.A., Karmakar,P., Opresko,P.L., Piotrowski,J., Dianova,I., Dianov,G.L. and Bohr,V.A. (2001) Werner syndrome protein interacts with human flap endonuclease 1 and stimulates its cleavage activity. *EMBO J.*, **20**, 5791–5801.
31. Parker,J.L. and White,M.F. (2005) The endonuclease Hje catalyses rapid, multiple turnover resolution of Holliday junctions. *J. Mol. Biol.*, **350**, 1–6.

32. David-Cordonnier,M.H., Laval,J. and O'Neill,P. (2001) Recognition and kinetics for excision of a base lesion within clustered DNA damage by the *Escherichia coli* proteins Fpg and Nth. *Biochemistry*, **40**, 5738–5746.
33. Tom,S., Henricksen,L.A. and Bambara,R.A. (2000) Mechanism whereby proliferating cell nuclear antigen stimulates flap endonuclease 1. *J. Biol. Chem.*, **275**, 10498–10505.
34. Liu,Y., Zhang,H., Veeraraghavan,J., Bambara,R.A. and Freudenreich,C.H. (2004) *Saccharomyces cerevisiae* flap endonuclease 1 uses flap equilibration to maintain triplet repeat stability. *Mol. Cell. Biol.*, **24**, 4049–4064.
35. Gordenin,D.A., Kunkel,T.A. and Resnick,M.A. (1997) Repeat expansion—all in a flap? *Nature Genet.*, **16**, 116–118.
36. Murante,R.S., Rust,L. and Bambara,R.A. (1995) Calf 5′ to 3′ exo/endonuclease must slide from a 5′ end of the substrate to perform structure-specific cleavage. *J. Biol. Chem.*, **270**, 30377–30383.
37. Wang,W. and Bambara,R.A. (2005) Human Bloom protein stimulates flap endonuclease 1 activity by resolving DNA secondary structure. *J. Biol. Chem.*, **280**, 5391–5399.
38. Huang,S., Beresten,S., Li,B., Oshima,J., Ellis,N.A. and Campisi,J. (2000) Characterization of the human and mouse WRN 3′→5′ exonuclease. *Nucleic Acids Res.*, **28**, 2396–2405.
39. Barnes,C.J., Wahl,A.F., Shen,B., Park,M.S. and Bambara,R.A. (1996) Mechanism of tracking and cleavage of adduct-damaged DNA substrates by the mammalian 5′- to 3′-exonuclease/endonuclease RAD2 homologue 1 or flap endonuclease 1. *J. Biol. Chem.*, **271**, 29624–29631.
40. Bornarth,C.J., Ranalli,T.A., Henricksen,L.A., Wahl,A.F. and Bambara,R.A. (1999) Effect of flap modifications on human FEN1 cleavage. *Biochemistry*, **38**, 13347–13354.
41. Joyce,C.M. and Steitz,T.A. (1994) Function and structure relationships in DNA polymerases. *Annu. Rev. Biochem.*, **63**, 777–822.
42. Sporbert,A., Domaing,P., Leonhardt,H. and Cardoso,M.C. (2005) PCNA acts as a stationary loading platform for transiently interacting Okazaki fragment maturation proteins. *Nucleic Acids Res.*, **33**, 3521–3528.
43. Hasan,S., Stucki,M., Hassa,P.O., Imhof,R., Gehrig,P., Hunziker,P., Hubscher,U. and Hottiger,M.O. (2001) Regulation of human flap endonuclease-1 activity by acetylation through the transcriptional coactivator p300. *Mol. Cell*, **7**, 1221–1231.
44. Sharma,S., Sommers,J.A., Gary,R.K., Friedrich-Heineken,E., Hubscher,U. and Brosh,R.M.Jr (2005) The interaction site of Flap Endonuclease-1 with WRN helicase suggests a coordination of WRN and PCNA. *Nucleic Acids Res.*, **33**, 6769–6781.
45. Moore,H., Greenwell,P.W., Liu,C.P., Arnheim,N. and Petes,T.D. (1999) Triplet repeats form secondary structures that escape DNA repair in yeast. *Proc. Natl Acad. Sci. USA*, **96**, 1504–1509.
46. Ruggiero,B.L. and Topal,M.D. (2004) Triplet repeat expansion generated by DNA slippage is suppressed by human flap endonuclease 1. *J. Biol. Chem.*, **279**, 23088–23097.
47. Sharma,S., Sommers,J.A. and Brosh,R.M.Jr (2004) *In vivo* function of the conserved non-catalytic domain of Werner syndrome helicase in DNA replication. *Hum. Mol. Genet*, **13**, 2247–2261.
48. Sharma,S., Otterlei,M., Sommers,J.A., Driscoll,H.C., Dianov,G.L., Kao,H.I., Bambara,R.A. and Brosh,R.M.Jr (2004) WRN helicase and FEN-1 form a complex upon replication arrest and together process branchmigrating DNA structures associated with the replication fork. *Mol. Biol. Cell*, **15**, 734–750.
49. von Kobbe,C., Thoma,N.H., Czyzewski,B.K., Pavletich,N.P. and Bohr,V.A. (2003) Werner syndrome protein contains three structure-specific DNA binding domains. *J. Biol. Chem.*, **278**, 52997–53006.
50. Lee,J.W., Kusumoto,R., Doherty,K.M., Lin,G.X., Zeng,W., Cheng,W.H., von Kobbe,C., Brosh,R.M.Jr, Hu,J.S. and Bohr,V.A. (2005) Modulation of Werner syndrome protein function by a single mutation in the conserved RecQ domain. *J. Biol. Chem.*, **280**, 39627–39636.